

## Thermal Decomposition Kinetic and Flame Retardancy of CaCO<sub>3</sub> Filled Recycled Polyethylene Terephthalate/Recycled Polypropylene Blend

Supaphorn Thumsorn, Kazushi Yamada, Yew Wei Leong, Hiroyuki Hamada

Department of Advanced Fibro-Science, Kyoto Institute of Technology, Japan

Correspondence to: S. Thumsorn (E-mail: supaphornthumsorn@yahoo.com)

**ABSTRACT:** The flammability and thermal decomposition kinetics of recycled polyethylene terephthalate (RPET)/recycled polypropylene (RPP) blends filled with CaCO<sub>3</sub> were investigated. The thermal decomposition kinetics were determined by using various models such as the Flynn-Wall-Ozawa, Kissinger, and Kim-Park, which would define the thermal stability of the blends through the determination of their decomposition activation energies. Meanwhile, the flammability of the materials was also determined through the limiting oxygen index (LOI) method. It was found that blends with higher RPP content or contain CaCO<sub>3</sub> exhibited higher resistance to thermal degradation judging from their higher activation energies. Furthermore, it was found that the isoconversion kinetic of the Flynn-Wall-Ozawa model could provide a better estimation of the decomposition activation energy at each stage of degradation.

© 2012 Wiley Periodicals, Inc. *J. Appl. Polym. Sci.* 000: 000–000, 2012

**KEYWORDS:** thermal decomposition kinetic; activation energy; RPET/RPP blend; CaCO<sub>3</sub>; flame retardance

Received 26 October 2010; accepted 8 March 2012; published online

DOI: 10.1002/app.37673

### INTRODUCTION

Degradation of polymers is generally affected by physical and chemical environment such as UV light, heat, acid or solvent. Degradation of polymeric products usually occurs from the surface towards the internal regions through chain scission and later erosion, which causes significant discoloration, reduction in mechanical performance and mass loss. These degradation mechanisms would also occur during melt processing where heat, moisture and oxygen are present. The understanding of degradation mechanism and kinetics is especially important during recycling of thermoplastics since they would directly affect processing conditions, final properties and application of these materials. Thermal decomposition kinetic studies could provide useful information on the thermal decomposition behavior and the mechanisms involved through the expressions of various kinetic parameters. These kinetic parameters can be investigated by applying various kinetic models that define the thermal decomposition of materials under specific conditions.<sup>1–11</sup>

One of the most recycled thermoplastics is polyethylene terephthalate (PET) since it constitutes a large portion of post consumer wastes due to its wide usage in beverage and food packaging applications. For example, the annual consumption of PET drinking bottles in Japan, in 2009, was 50% higher than in the past few years.<sup>12</sup> Therefore, recycling of waste PET bottles

offers a possible solution to reduce landfill waste. Blending of recycled PET bottles (RPET) with their polypropylene-based caps (RPP) would further reduce the costs incurred to separate these components prior to recycling. Moreover, it is important to emphasize that recycled materials would definitely be more attractive should they exhibit comparable or superior mechanical performance, thermal stability and processability as compared to neat materials. Therefore, there is a need to upgrade these materials by incorporation of compatibilizers, stabilizers, or reinforcements. In fact, it has been shown that blending of RPET and RPP with proper compatibilization yielded tougher and more thermally stable material.<sup>13–15</sup> However, due to the low stiffness of the RPP phase and the compatibilizer, a significant reduction in modulus of the blends was noted.

Another property that is considered important when it comes to recycling of PET is its flammability since this material is often made into textiles and fabrics that are used in upholstery and carpeting. Therefore, it is flame retardant polymeric materials typically possess traits such as the ability to prevent extensive combustion, increase ignition resistance, and reduce the spreading of flame.<sup>16–24</sup> Flame retardant materials for thermoplastics can be classified as halogenated compounds, phosphorous compounds, metallic oxides and inorganic fillers. The mechanisms of flame retardant are endothermic degradation such as magnesium and aluminum hydroxides, dilution of filler by fillers such

© 2012 Wiley Periodicals, Inc.

as talc or calcium carbonate, thermal shielding by using intumescent additive, or gas phase radical quenching such as brominated and chlorinated materials.<sup>19</sup> In general, halogenated are widely used as flame retardant material which burning of this material cause toxicity whereas the other should be considered on the reduction of mechanical properties when it presents in the composite.

In this study, since it is important to retain good thermal stability of RPET/RPP blends, the degradation kinetics of the RPET/RPP blends were investigated by using several decomposition models. CaCO<sub>3</sub> was used as a low-cost and non-toxic filler in RPET/RPP blends in order to improve its processability, rigidity and thermal stability. Furthermore, the viability of using CaCO<sub>3</sub> as a flame retardant for RPET/RPP blends was elucidated.

## EXPERIMENTAL

### Materials

Both recycled polyethylene terephthalate (RPET) (viscosity average molecular weight = 23,131 g/mol)<sup>25</sup> and recycled polypropylene (RPP) (MFI = 15 g/10 min) in the form of flake (from crushed waste bottles) were provided by Yasuda Sangyo (Japan). A finely ground commercial grade CaCO<sub>3</sub> (SOFTON 1200) with an average particle size of 1.8 μm was purchased from Bihoku Funaka Kogyo (Japan). A styrene-ethylene-butadiene-styrene base compound was used as compatibilizer, which was purchased from JSR Corporation (Japan). The ratio of RPET/RPP blend was set at 95/5 and 90/10. The content of CaCO<sub>3</sub> was varied at 10 and 20 wt %. The blends without compatibilizer and CaCO<sub>3</sub> were also prepared. The amount of the compatibilizer was fixed at 5 phr (part per hundred resins by weight). The composition of the blends was shown in Table I.

### Sample Preparation

The blends were compounded by using a single screw extruder (SRV-P70/62, Nihon Yuki, Japan). RPET was dried by using a dehumidifying drier at 120°C for 5 h before compounding. The extruder barrel temperature was set at 260–285°C and screw speed at 50 rpm. The blends were again dried at 120°C for 5 h in the oven before being injection molded into dumbbell specimens by using a Po Yuen UM50 injection molding machine for further characterization. The barrel temperature, injection speed, and mold temperature during injection molding were set at 280°C, 100 mm/s, and 30°C, respectively.

### Morphology Observation

Morphology of the blends was characterized from cryogenic fractured surface of the specimens by using a field emission scanning electron microscope (Hitachi, S-4200). Gold coating was sputtered onto the specimens for electron conductivity. The image J program was used to measure the size of the disperse phase particles, according to eqs. (1) and (2)

$$\text{Particlediameter} (d_i) = \sqrt{\frac{4 \times \text{area}}{\pi}} \quad (1)$$

$$\text{Numberaveragediameter} (d_n) = \frac{\sum N_i d_i}{\sum N_i} \quad (2)$$

where  $N_i$  is number of particle, which having diameter  $d_i$ .

**Table I.** Materials Composition of Unfilled and CaCO<sub>3</sub> Filled 95/5 Blend and 90/10 Blend

RPET/RPP	RPET (wt %)	RPP (wt %)	CaCO <sub>3</sub> (wt %)	SEBS (phr)
95/5	95	5	0	0
			0	5
			10	
90/10	90	10	0	0
			0	5
			10	
			20	

### Moisture Content

Moisture content was carried out according to ASTM D280. The dumbbell specimen was initially weighed, then heated at 110°C for 2 h, and cooled in the desiccator. The percentage of moisture content in the specimen was calculated by the following equation:

$$\text{Moisturecontent (\%)} = \frac{\text{initialweight} - \text{driedweight}}{\text{initialweight}} \times 100 \quad (3)$$

### Thermal Stability and Decomposition Kinetic

Thermogravimetric analysis (TGA) was performed by using a TA Instruments TGA2950 analyzer to elucidate the thermal decomposition kinetics of CaCO<sub>3</sub> filled blends. The samples weighing between 3 and 5 mg was subjected to heating rates of 2, 5, 10, and 20°C/min in nitrogen and air.

TGA data provides information for the calculation of the conversion of sample ( $\alpha$ ) during decomposition. At linear heating rate  $\alpha$  is defined as

$$\alpha = \frac{m_0 - m_T}{m_0 - m_{\text{final}}} \quad (4)$$

where  $m_0$  is the initial mass,  $m_T$  is the mass at decomposition temperature, and  $m_{\text{final}}$  is the mass at final decomposition reaction.

The activation energy of thermal decomposition kinetic for these specimens was then determined by using Flynn and Wall, Kissinger, and Kim-Park methods for kinetic studies. These methods can be applied for studying thermal degradation and decomposition kinetic of polymeric materials based on the Arrhenius equation<sup>6–8,10</sup>

$$\frac{d\alpha}{dt} = A \exp\left(\frac{-E_a}{RT}\right) f(\alpha) \quad (5)$$

where  $\alpha$  is the fraction of weight loss or conversion value of decomposition,  $A$  is the pre-exponential factor,  $E_a$  is activation energy,  $R$  is universal gas constant,  $n$  is reaction order,  $t$  is time, and  $T$  is temperature.

For thermal degradation with the linear heating rate is defined as

$$\beta = \frac{dT}{dt} \quad (6)$$

where  $\beta$  is the heating rate (K/min).

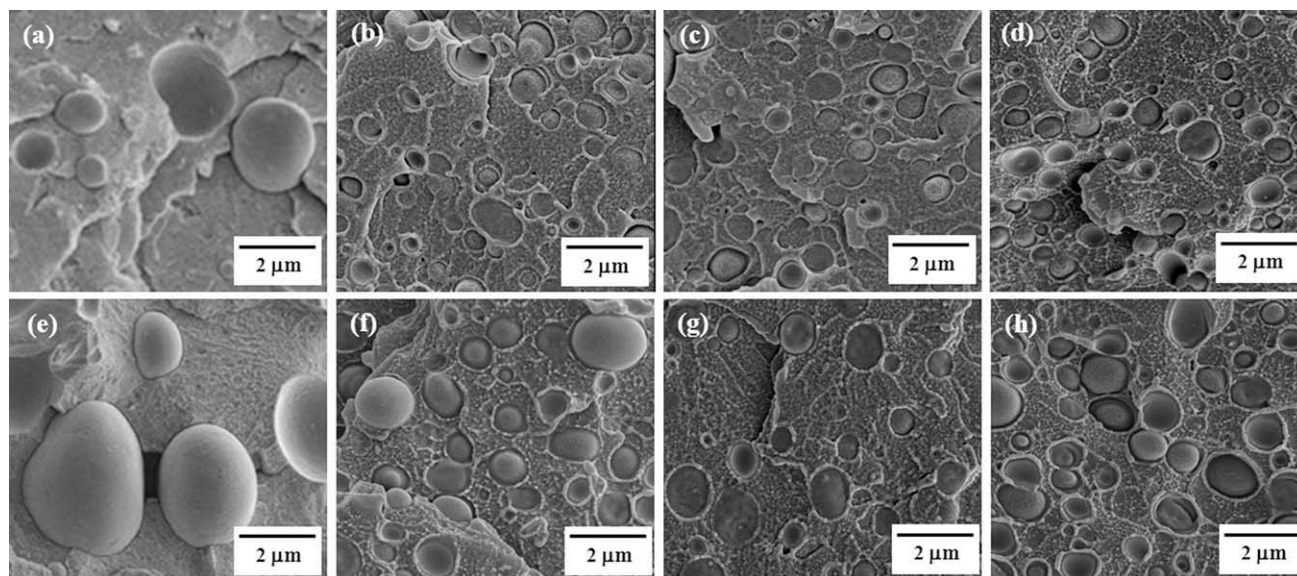


**Figure 1.** SEM photographs of 95/5 blend (a) uncompatibilized and compatibilized blends with (b) 0 wt %, (c) 10 wt %, (d) 20 wt %  $\text{CaCO}_3$ , and 90/10 blend (e) uncompatibilized and compatibilized blends with (f) 0 wt %, (g) 10 wt %, and (h) 20 wt %  $\text{CaCO}_3$ .

For the kinetic study of non-isothermal experimental, eq. (3) is rewritten by

$$\frac{d\alpha}{dT} = \frac{A}{\beta} \exp\left(\frac{-E_a}{RT}\right) f(\alpha) \quad (7)$$

According to eq. (7), differential and integral methods were applied for the calculation of thermal degradation/decomposition kinetic parameter.<sup>8,10</sup> The decomposition kinetic parameters including activation energy ( $E_a$ ), reaction order ( $n$ ), and pre-exponential factor ( $A$ ) can represent the thermal stability and present an idea as to the decomposition mechanism of the samples. Apart from the aforementioned methods that were all using multiple heating rates to determine the decomposition kinetics, methods utilizing only single heating rate such as Friedman, Freeman-Carroll, and Chang are also available.<sup>8,10</sup> However, a composite material such as those used in this study could undergo multiple degradation stages. Therefore, multiple heating rate methods were selected to accurately determine the degradation kinetics and to better understand the degradation mechanisms involved.

#### Limiting Oxygen Index

Flame retardancy of the materials was characterized by using the limiting oxygen index (LOI) [ONI (oxygen index) meter, Suga Test Instruments, Japan] according to JIS K 7201-2, specimen type IV. The specimens bearing geometries of 80 mm long,  $6.5 \pm 0.5$  mm wide, and  $3 \pm 0.5$  mm thick were obtained from the middle section of the injection molded dumbbells. The minimum concentration of oxygen in a flowing mixture of oxygen and nitrogen needed to continuously burn the sample for over 3 min or for a length of more than 50 mm was determined to be the LOI.

#### Mechanical Properties

Tensile test were performed by using an Instron 4206 universal testing machine according to standards ASTM D638. The gauge length was 115 mm at an extension rate of 20 mm/min.

Izod impact strength was determined for 2 mm-deep notched specimens, which was cut from the parallel regions of the dumbbell specimens. The test was conducted by using a Toyo Seiki Izod impact tester according to ASTM D256 with a pendulum of 5.50 J.

## RESULTS AND DISCUSSION

### Morphology of Unfilled and $\text{CaCO}_3$ Filled RPET/RPP Blend

Figure 1 shows SEM photographs of uncompatibilized blend and compatibilized of 95/5 and 90/10 blends filled with 0–20 wt %  $\text{CaCO}_3$ . The morphological characteristics of incompatible system with a poor dispersion of RPP dispersed phase could be observed in Figure 1(a, e) for uncompatibilized 95/5 and 90/10 blends, respectively. It was due to the high interfacial tension between different polymer blends resulting in the coalescence of the minor phase during the compounding. The morphological characteristics of the compatibilized blends were significantly different. A reduction in RPP dispersed phase sizes was evident with the incorporation of compatibilizer as shown in Figure 1(b–d) and (g–h) for the compatibilized 95/5 blends and 90/10 blends, respectively. The compatibilizer provided an important role on reduce the interfacial tension between two different polymer blends, which obtained the small size of RPP dispersed particles on the RPET matrix. A better dispersion and improved adhesion at the RPP/RPET interface was also noted,<sup>14,26,27</sup> which considerably from the role of compatibilizer. The RPP dispersed phase particles size of 95/5 blends are 3.18, 0.65, 0.48, and 0.41  $\mu\text{m}$  for uncompatibilized and compatibilized blend with 0, 10, and 20 wt %  $\text{CaCO}_3$ , respectively. On the other hand, the RPP dispersed particle of 90/10 blends were larger, which the particle size are 5.30, 0.72, 0.61, and 0.62  $\mu\text{m}$  for uncompatibilized and compatibilized blend with 0, 10, and 20 wt %  $\text{CaCO}_3$ , respectively. The higher content of RPP in 90/10 blends resulting in larger RPP dispersed particle, which the reduction of the interfacial tension from the compatibilizer

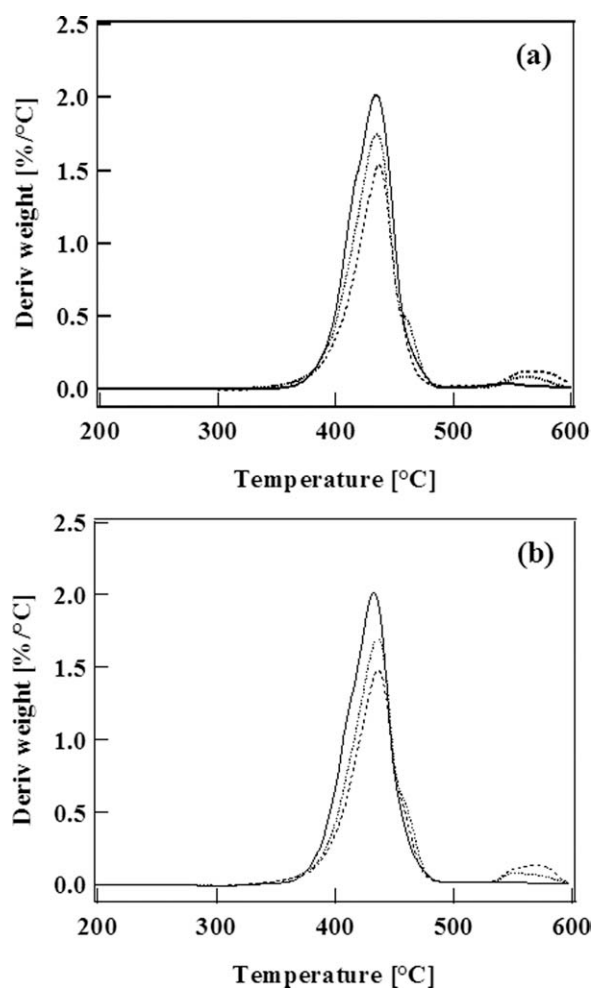


**Figure 2.** TGA derivative thermogram of unfilled and  $\text{CaCO}_3$  filled of (a) 95/5 blend and (b) 90/10 blend in nitrogen at  $10^\circ\text{C}/\text{min}$ .

might not be enough for these blends. The incorporation of  $\text{CaCO}_3$  presented a smaller RPP dispersed particle in both 95/5 blends and 90/10 blends. It could be due to  $\text{CaCO}_3$  would breakage RPP dispersed phase during compounding. Generally, the morphology of the blends is significantly effect on physical and mechanical properties of the blends.<sup>14,15</sup> The smaller

dispersed phase size would obtain greater properties. Therefore, this research is focus on the effect of  $\text{CaCO}_3$  on the properties of compatibilized RPET/RPP blends.

#### Thermal Stability and Degradation Temperature

Thermogravimetric analysis (TGA) is a useful technique to evaluate the decomposition kinetics of the composites as a function of temperature and time. The TGA thermograms of the various contents of  $\text{CaCO}_3$  filled blends heated in nitrogen and air are presented in Figure 2 whereas the onset and peak degradation temperatures are compiled in Tables II and III, respectively. The thermograms of  $\text{CaCO}_3$  filled blends featured in Figure 2 show single-step degradation when they were exposed to nitrogen. The residual corresponds to the  $\text{CaCO}_3$  content and some ash from the polymer. The onset degradation temperature of the blend would shift slightly to a higher temperature with increasing  $\text{CaCO}_3$  content. It indicates that  $\text{CaCO}_3$  has the potential to improve the thermal degradation resistance of the blend. In addition, the derivative peak intensities of the thermograms decreased with the presence of  $\text{CaCO}_3$ , which implied a reduction rate of degradation in the blends. On the other hand, a two-step degradation profile could be observed when the specimens were exposed to air, as shown in Figure 3. An oxidative atmosphere accelerated the degradation of the polymers, which could be noted from their lower onset degradation temperatures as compared to those exposed to nitrogen. It is interesting to note that upon incorporation of  $\text{CaCO}_3$ , the onset shifted towards a higher temperature indicating better thermal stability. Meanwhile, the appearance of a second step in the thermogram corresponds to the conversion of the ash to  $\text{CO}_2$  or  $\text{CO}$ .<sup>23</sup> The incorporation of  $\text{CaCO}_3$  resulted in the decomposition of the ash at lower temperatures, which highlights the catalytic effect of the filler.<sup>23,24</sup> Tables II and III tabulate the onset and peak degradation temperatures of unfilled and  $\text{CaCO}_3$  filled RPET/RPP blends. Both onset and peak degradation temperature increased when increasing  $\text{CaCO}_3$  contents. However, the degradation temperatures are almost unchanged between 95/5 and 90/10 blends.

Figure 4(a, b) shows the overlay of TGA thermograms of 20 wt %  $\text{CaCO}_3$  filled 95/5 blend specimens exposed to different heating rates in nitrogen and air atmosphere. The weight loss profiles shifted to higher temperature while the derivative peak

**Table II.** Onset Degradation Temperature ( $T_{d \text{ onset}}$ ) at 5% Weight Loss of Unfilled and  $\text{CaCO}_3$  Filled 95/5 Blend and 90/10 Blend

RPET/RPP blend	Heating rate ( $^\circ\text{C}/\text{min}$ )	$T_{d \text{ onset}}$ ( $^\circ\text{C}$ ) $\text{N}_2$			$T_{d \text{ onset}}$ ( $^\circ\text{C}$ ) air		
		$\text{CaCO}_3$ content (wt %)			$\text{CaCO}_3$ content (wt %)		
		0	10	20	0	10	20
95/5	2	366.2	366.0	367.4	324.5	339.1	344.3
	5	382.2	381.2	383.5	347.5	355.8	357.7
	10	394.3	392.9	396.4	370.0	371.1	371.9
	20	403.9	403.7	407.5	391.2	393.8	395.1
90/10	2	365.6	368.0	368.8	336.6	335.5	340.3
	5	380.9	379.6	385.1	356.6	355.9	356.0
	10	393.7	395.3	396.7	373.7	367.0	364.8
	20	405.3	407.0	408.7	390.5	380.5	381.3

**Table III.** Peak Degradation Temperature of Unfilled and CaCO<sub>3</sub> Filled 95/5 Blend and 90/10 Blend

RPET/RPP blend	Heating rate (°C/min)	$T_{d \text{ peak}} \text{ (}^\circ\text{C)} \text{ N}_2$			$T_{d \text{ peak}} \text{ (}^\circ\text{C)} \text{ air}$		
		CaCO <sub>3</sub> content (wt %)			CaCO <sub>3</sub> content (wt %)		
		0	10	20	0	10	20
95/5	2	405.3	404.9	405.1	390.0	397.7	399.2
	5	422.0	422.1	422.0	410.0	416.9	416.9
	10	434.9	435.5	437.0	430.0	433.7	436.3
	20	443.8	447.5	450.0	441.5	446.1	437.6
90/10	2	402.3	407.2	407.6	394.1	402.8	399.9
	5	419.6	423.9	424.2	409.9	417.4	421.1
	10	432.6	436.1	436.6	426.6	431.3	429.2
	20	446.0	448.4	450.3	425.5	446.1	451.9

temperature increased although the peak height decreased with increasing heating rates. It was caused by the heat capacity of the specimens whereby the heating rate of the polymer was not in equilibrium to the heating rate of the furnace.<sup>3</sup> It can be noted that the heating rate would significantly affect the decomposition characteristics of the specimens.

### Thermal Decomposition Kinetic

Classical multiple-heating-rate thermal degradation kinetic models such as Flynn-Wall-Ozawa, Kissinger and Kim-Park were studied and summarized by various researchers.<sup>1,2,5-11,28</sup> These models, while basing the degradation kinetic calculations on the Arrhenius equation, would each have some differing approaches towards interpreting the degradation mechanism of the materials either monotonic or multi-components system. However, there is lack of a research on thermal decomposition kinetic of recycled polymer blends. Flynn and Wall<sup>6-8,10</sup> is a simple model that provides the activation energy for thermal decomposition,  $E_a$  at every stage of specimen weight loss during TGA. Therefore, the step or mechanism of decomposition, especially for composite materials or polymer blends, can be elucidated more accurately by using this method.<sup>6</sup>

### Thermal Decomposition Kinetic from Flynn-Wall-Ozawa

The decomposition kinetic information of Flynn and Wall method was developed by Ozawa to form a kinetic equation known as the Flynn-Wall-Ozawa (FWO) model,<sup>2,6,28,29</sup> which is derived from the integral method of eq. (7). The FWO model involves measuring the degradation temperatures corresponding to values of weight loss during the decomposition ( $\alpha$ ). The eq. (7) is integrated with  $\alpha = 0$  at  $T = T_0$  (the initial temperature) and can be assigned by using the Doyle approximation.<sup>30,31</sup> FWO model is expressed in the form of

$$\log \beta = \log \frac{AE_a}{f(\alpha)R} - 2.315 - \frac{0.457E_a}{RT} \quad (8)$$

where  $f(\alpha)$  is a function of the fraction of weight loss or a conversion function of decomposition kinetic,  $f(\alpha) = (1 - \alpha)^n$ ;  $n = 1$ ,  $E_a$  is decomposition activation energy (J/mol),  $A$  is the pre-exponential factor,  $R$  is a universal gas constant (8.314 J/mol K),  $\beta$  is heating rate, and  $T$  is temperature (K). This integral method allows for  $E/RT > 20$ . At constant heating rate,  $E_a$  can be calculated from the

slope of logarithm heating rate as a function of inverse temperature and can be expressed as

$$E_a = - \left( \frac{R}{0.457} \right) \left( \frac{d(\log \beta)}{d(1/T)} \right) \quad (9)$$

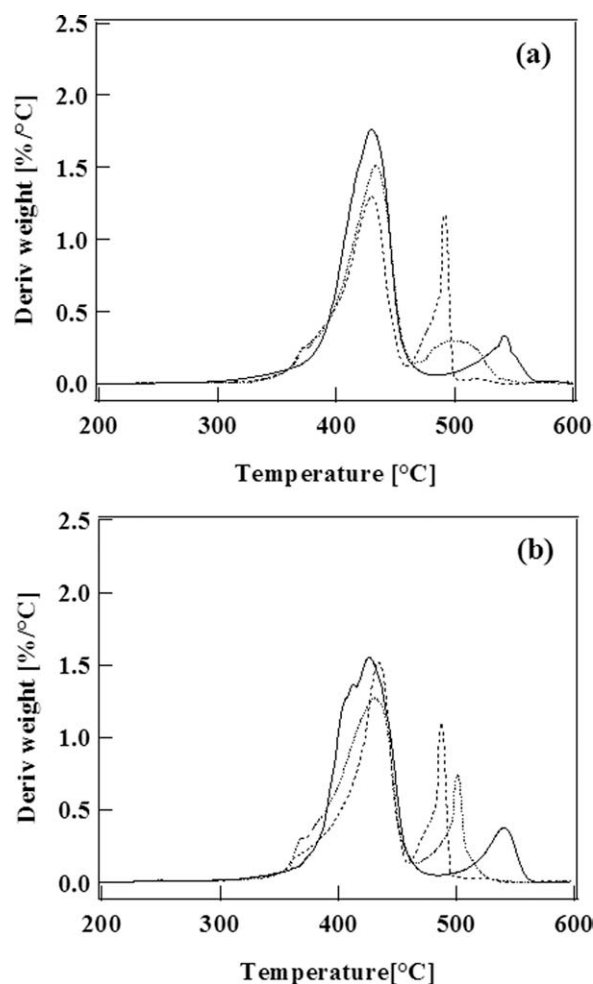


**Figure 3.** TGA derivative thermogram of unfilled and CaCO<sub>3</sub> filled of (a) 95/5 blend and (b) 90/10 blend in air at 10°C/min.

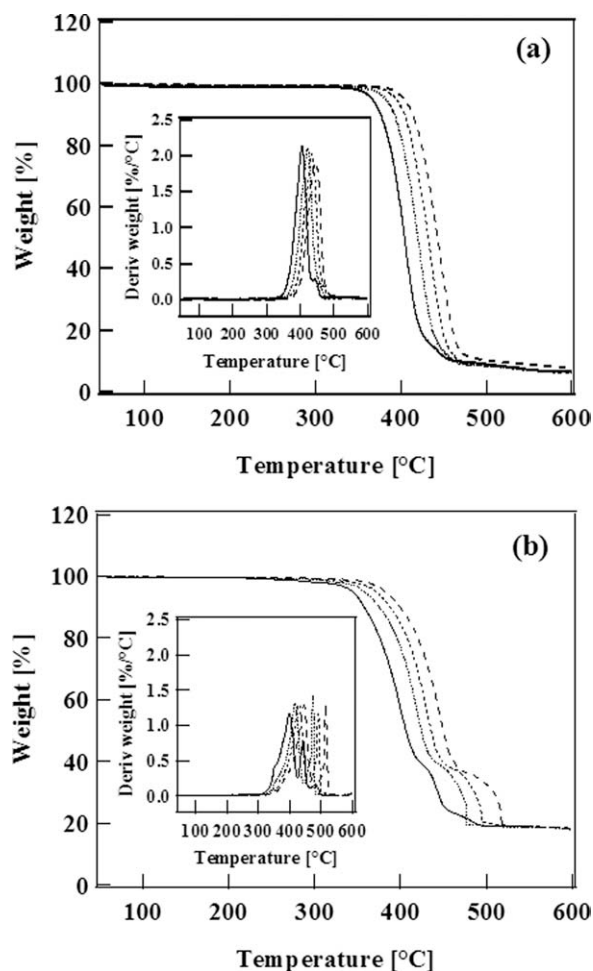


**Figure 4.** TGA Thermogram of 95/5 blend filled with 20 wt %  $\text{CaCO}_3$  at different heating rate in (a) nitrogen and (b) air.

From the logarithmic plots of heating rate as a function of inverse temperature in Figure 5 the slopes were used to calculate the activation energy at stages of decomposition based on sample weight loss. The Flynn-Wall-Ozawa (FWO) plots are straight and independent of heating rate, which corresponds to first order reaction by  $f(\alpha) = (1-\alpha)$ .<sup>9</sup> The activation energy can be calculated from the slope of the plots and the results are shown in Figures 6 and 7. The summary of  $E_a$  of the filled blend at 5% ( $T_5$ ) and 50% ( $T_{50}$ ) weight loss is presented in Table IV. Figures 6 and 7 depict  $E_a$  at various weight loss of  $\text{CaCO}_3$  filled 95/5 and 90/10 blend in nitrogen and air, respectively. It can be seen that the  $E_a$  values of the filled blends were almost constant throughout the degradation process when they were exposed to nitrogen whereas a significant increment of  $E_a$  values could be observed when the specimens were degraded in the presence of oxygen in the air atmosphere. On the contrary, the different activation energies at the initial and later stages of degradation when the specimens were exposed to oxidative environment suggest that the specimens have undergone a two-step thermo-oxidative degradation as shown in Figures 6(b) and 7(b). From the results, the initial stage can be attributed to the degradation through oxidative degradation or depolymerization of low thermal stability of RPP. During thermal-oxidative degradation, heat

activated polymer chain breaking to free radical and oxygen generated hydroperoxide and resulted in chain scission of RPP component.<sup>5</sup> The following step can be attributed to the chain scission of RPET matrix at the ester linkages leading to formation of carboxylic acid and ester end groups.<sup>7,23,32</sup> From Table IV, the  $E_a$  values for thermal and thermo-oxidative degradation of 95/5 and 90/10 blends increased with increasing  $\text{CaCO}_3$  contents, which highlights the ability of  $\text{CaCO}_3$  to retard thermal decomposition of RPET/RPP blend. The  $E_a$  values of 90/10 blends were considerably higher than 95/5 blends, which would be accompanied on low  $E_a$  values of RPET and depended on morphology of the blends. The RPP dispersed phase size of 90/10 blends were larger, which presented smaller surface area for thermal decomposition reaction as compared to 95/5 blends. Therefore, 90/10 blends exhibited higher  $E_a$  values than 95/5 blends. It also revealed that the activation energies of thermal decomposition kinetic of the blends in air were lower than in nitrogen atmosphere, which was due to the accelerated thermo-oxidative degradation in the presence of oxygen in air atmosphere. It is interesting to note that the incorporation of  $\text{CaCO}_3$  significantly delayed thermo-oxidative degradation of the blends, which is indicated by the increasing  $E_a$  values especially at the initial stages of degradation as

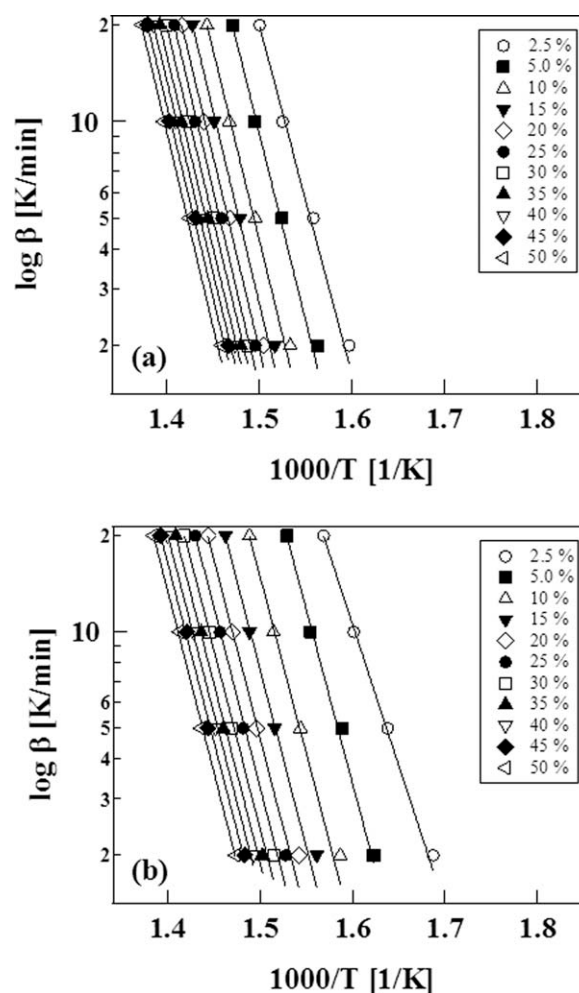


**Figure 5.** Flynn-Wall-Ozawa plots of 20 wt %  $\text{CaCO}_3$  filled 95/5 blend in (a) nitrogen and (b) air.

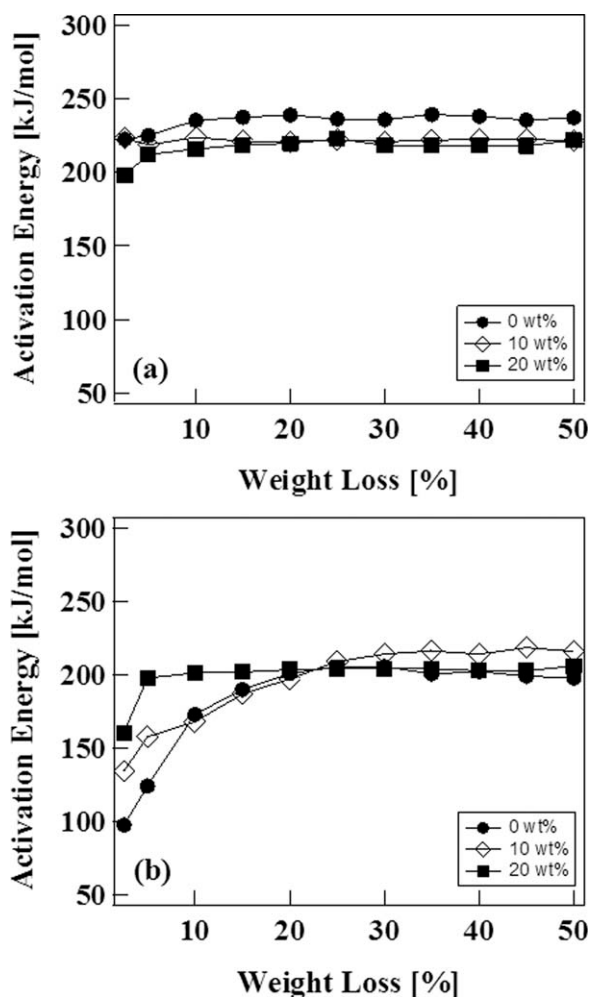


Figure 6. Activation energies of CaCO<sub>3</sub> filled 95/5 blend in (a) nitrogen and (b) air.

shown in Figures 6(b) and 7(b). Furthermore, CaCO<sub>3</sub> could act as an antioxidant to inhibit the oxidation of polymer as described by Traian et al.<sup>33</sup> Therefore, the FWO method was able to show that thermal degradation of the recycled blends occurred as a two-step process and oxidative degradation was dominant only at the early stages of decomposition.

**Thermal Decomposition Kinetic from Kissinger and Kim-Park**

The Kissinger and Kim-Park methods, on the other hand, would provide a single or apparent  $E_a$  value to characterize the entire thermal degradation process of the materials. Both methods would attempt the calculation of  $E_a$  based on the temperature at maximum rate of degradation.<sup>5,8,10,11</sup> The multiple heating rates were applied for these methods in order to characterizing the variation patterns of the peak derivative properties in term of representing a thermal decomposition at various stages of degradation.

The Kissinger model can be described as

$$\ln\left(\frac{\beta}{T_{dm}^2}\right) = \ln\left(\frac{AR}{E_a f(\alpha)}\right) - \frac{E_a}{RT_{dm}} \quad (10)$$

where  $f(\alpha) = n(1 - \alpha_m)^{n-1}$  and  $T_{dm}$  is the maximum peak degradation temperature at the maximum rate of thermal decomposition.

Meanwhile, the Kim-Park model has also been used for determining a single  $E_a$  value to describe the thermal degradation kinetics of unfilled and CaCO<sub>3</sub> filled RPET/RPP blend through the following equation

$$\ln \beta = \ln A + \ln\left(\frac{E_a}{R}\right) + \ln\left[1 - n + \left(\frac{n}{0.944}\right)\right] - 5.3305 - 1.0516\left(\frac{E_a}{RT_{dm}}\right) \quad (11)$$

Figure 8(a, b) shows the plot of  $\ln(\beta/T_{dm}^2)$  versus  $1/T_{dm}$  based on the Kissinger method and the plot of  $\ln \beta$  versus  $1/T_{dm}$  based on Kim-Park method, respectively. The slopes from the plots can be used to calculate the  $E_a$  values of unfilled and CaCO<sub>3</sub> filled RPET/RPP blends.

The Kissinger method was derived from the basic kinetic equation for heterogeneous chemical reactions which could be applied for calculating the thermal decomposition of these

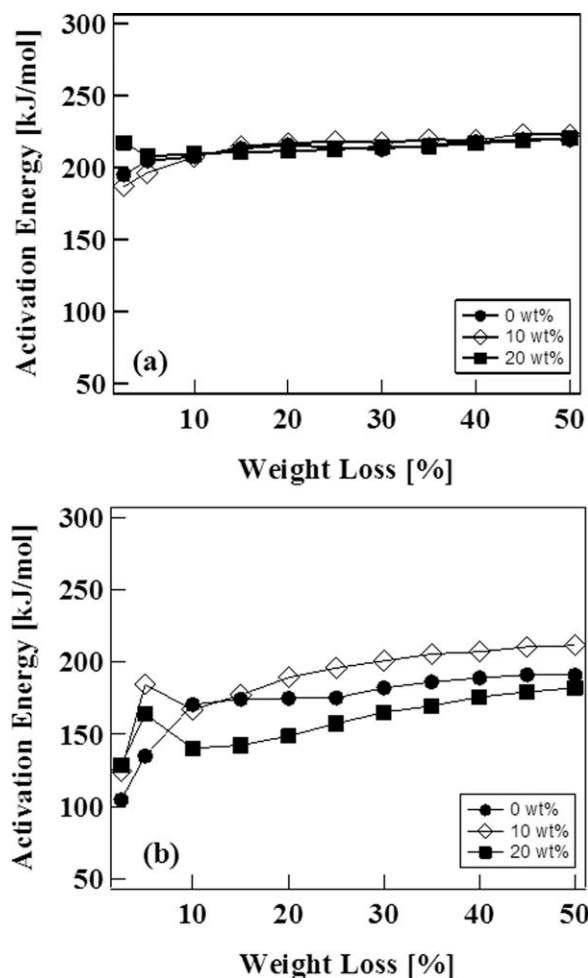


Figure 7. Activation energies of CaCO<sub>3</sub> filled 90/10 blend in (a) nitrogen and (b) air.

**Table IV.** Activation Energy from Flynn-Wall-Ozawa of the Materials, Unfilled, and CaCO<sub>3</sub> Filled 95/5 Blend and 90/10 Blend

Materials	CaCO <sub>3</sub> (wt %)	$E_a$ at $T_5$ (kJ/mol)		$E_a$ at $T_{50}$ (kJ/mol)	
		N <sub>2</sub>	Air	N <sub>2</sub>	Air
RPP		153.8	112.9	227.4	117.0
SEBS		202.0	117.1	227.8	139.3
RPET		201.7	80.0	214.0	120.3
CaCO <sub>3</sub>		176.6	243.5	174.0	166.1
95/5 Blend	0	225.1	124.2	237.1	198.0
	10	218.6	157.8	221.7	215.9
	20	212.2	201.8	221.9	213.5
90/10 Blend	0	204.9	134.9	219.6	191.0
	10	196.4	184.3	223.1	211.6
	20	208.1	178.4	220.9	162.7

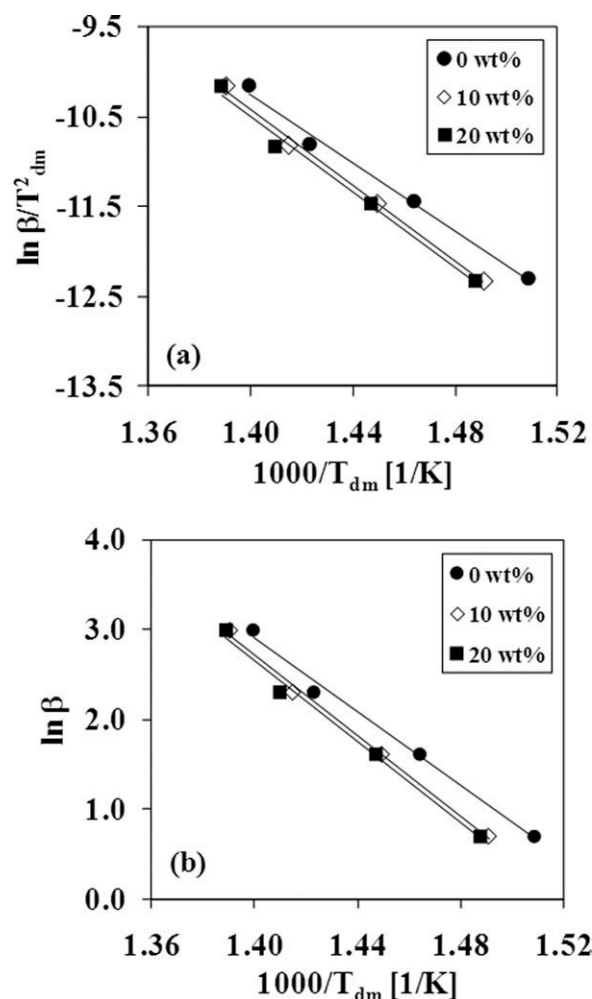
blends without the need to know the reaction order,  $n$ , or the conversion function,  $f(\alpha)$ .<sup>34</sup> On the other hand, the Kim-Park method can be applied through the determination of peak temperatures and heights of the derivative thermogravimetry (DTG) curves.<sup>11</sup> However, applying this method for thermal decomposition kinetic study should be carefully considered for complex reactions, which could cause disturbance of peak temperatures resulting in the overlapping of DTG curves. Furthermore, it should be noted that the activation energies of the blends can be influenced by various factors such as the kinetic methods, the sample mass and size, and the operating conditions.<sup>3,6</sup>

Decomposition kinetics from the Kissinger and Kim-Park models were calculated from the intensity of degradation temperature peak, which represent the sum of the activation energies of chemical reactions and physical processes during thermal decomposition of a composite.<sup>34</sup> The activation energy from the peak temperature could be attributed to weight loss and major decomposition from RPET matrix degradation. Tables V and VI compare the  $E_a$  values of unfilled and CaCO<sub>3</sub> filled RPET/RPP blends determined from the Kissinger and Kim-Park models when degraded in nitrogen and air, respectively. The results reveal that the  $E_a$  values of unfilled and CaCO<sub>3</sub> filled RPET/RPP blends were quite similar. However, higher  $E_a$  values were noticeable generated in 90/10 blends than in 95/5 blends irrespective of whether they were degraded in nitrogen or air. It should be noted that RPP would degrade at a substantially higher temperature without the presence of oxygen. In addition, the dispersion of the RPP phase is quite homogeneous and the RPET could act as an effective oxygen barrier to protect the RPP phase from thermo-oxidative degradation resulting in higher  $E_a$  values in 90/10 blends. Furthermore, the RPP dispersed phase sizes of 90/10 blends were larger, which presented smaller surface area for thermal decomposition reaction of these blends. The incorporation of high thermal resistance filler CaCO<sub>3</sub> would further increased the  $E_a$  of the blends, which highlights the ability of CaCO<sub>3</sub> to retard thermo-oxidative degradation of the blends. It could note that the residual during thermal decomposition of CaCO<sub>3</sub> was form as a layer, which

could be trapped free radicals to prevent them from attacking other parts of the polymer molecules,<sup>6,35</sup> thus preventing extensive thermo-oxidative degradation. The comparison of activation energies determined from various kinetic methods and the mechanism behind the thermal decomposition of the blends will be discussed next.

#### Activation Energy and Thermal Decomposition Mechanism

The blends in this study are multi-components consisted of recycled polymer including RPET and RPP, which were compatibilized by SEBS copolymer while CaCO<sub>3</sub> was incorporated as an inorganic filler.  $E_a$  values of each component and the blends are tabulated in Table IV, which calculated from Flynn-Wall-Ozawa method. The results of activation energy of RPET, PP, and CaCO<sub>3</sub> from this study are reliable and correspond with the literature studies.<sup>1,4,8,36</sup> The activation energies of the blends were higher than the individual components, which could be due to the need of more energy to overcome the bonding between the filler and the blend matrix during thermal decomposition. The presence of CaCO<sub>3</sub> in the blend would be a barrier to prevent diffusion of volatile decomposition products.<sup>37</sup>

**Figure 8.** (a) Kissinger plot and (b) Kim-Park plot of CaCO<sub>3</sub> filled 95/5 blend in air.



**Table V.** Activation Energy from Kissinger and Kim-Park Model of Unfilled and CaCO<sub>3</sub> Filled 95/5 Blend and 90/10 Blend in Nitrogen

RPET/RPP blend	CaCO <sub>3</sub> (wt %)	Kissinger		Kim-Park	
		$E_a$ (kJ/mol)	$r$	$E_a$ (kJ/mol)	$r$
95/5	0	225.0	0.9911	225.0	0.9919
	10	195.3	0.9900	196.8	0.9991
	20	206.4	0.9986	207.3	0.9987
90/10	0	201.2	0.9998	202.3	0.9998
	10	209.8	0.9999	210.6	0.9999
	20	216.3	0.9993	216.7	0.9994

Thermal stability of RPET/RPP blends was enhanced by the incorporation of CaCO<sub>3</sub>, which would provide better processability during recycling, which indicated by the increment of  $E_a$  values in CaCO<sub>3</sub> filled blends. The  $E_a$  values obtained through the Flynn-Wall-Ozawa method represent a step-by-step account of the thermal decomposition process, which was especially useful to understand the kinetics of major changes in multi-component materials. Meanwhile, the Kissinger and Kim-Park methods provided a summation of  $E_a$  values of thermal decomposition reaction, which these  $E_a$  values were corresponding to 40–50% weight loss.  $E_a$  values from the FWO model were higher than the Kissinger and Kim-Park methods when they were compared during the major stage of degradation (at 50% weight loss). It was due to the calculation of  $E_a$  from the peak degradation temperature using the Kissinger and Kim-Park models may have neglected some of the decomposition reactions at other temperatures. However, the Kissinger and Kim-Park methods are useful to provide just one  $E_a$  value as an indicator for thermal degradation resistance of a monotonic material, which are not expected to degrade at multiple stages. These results indicated the effect of kinetic method on calculated activation energy of kinetic parameter. However, the activation energy is similar when calculated from various kinetic techniques that applied in this study. Moreover,  $E_a$  from these three kinetic methods exhibited reliance on described thermal decomposition kinetics at first order reaction of the unfilled and filled RPET/RPP blend as the thermal decomposition occurred from an individual component and values of the correlation coefficient ( $r$ ) were greater than 0.99.<sup>6</sup> The activation energy from kinetic study could be considered

as minimum energy for thermal decomposition reaction of the recycled blends. The possible mechanism and kinetic parameters of multi-component for thermal decomposition in this study would clearly explain by using the Flynn-Wall-Ozawa method.

#### Flame Retardant Property of Unfilled and CaCO<sub>3</sub> Filled RPET/RPP Blend

The flammability of a polymer is dependent on the length of its hydrocarbon structure, which would decompose into fragments at pyrolysis temperature. Unfilled RPET/RPP blends are flammable with a hot and smoked flame of aromatic burning, accompanied by melting and then dripping or flowing of the molten polymer blend. This flammability of the blends would significantly limit their applications. The incorporation of flame retarding material could therefore be a sensible and practical approach to increase the ignition resistance of the blend and reduce the rate of flame propagation. Flame retardant property of CaCO<sub>3</sub> filled RPET/RPP blend was investigated by measuring the limiting oxygen index (LOI), which is defined as the minimum concentration of oxygen in an oxygen-nitrogen mixture, required to just support downward burning of a vertically mounted test specimen. Hence, higher LOI values represent better flame retardancy of the material. There are four different categories of materials based on LOI values including: (1) flammable materials with LOI less than 21%; (2) slow burning materials with LOI between 21 and 28%; (3) self-extinguishing materials with LOI greater than 28% and non-flammable materials with LOI higher than 35%.<sup>17</sup> Table VII shows the LOI values of RPET/RPP blends with various contents of CaCO<sub>3</sub>. It can be seen that the LOI values of the unfilled and filled blends

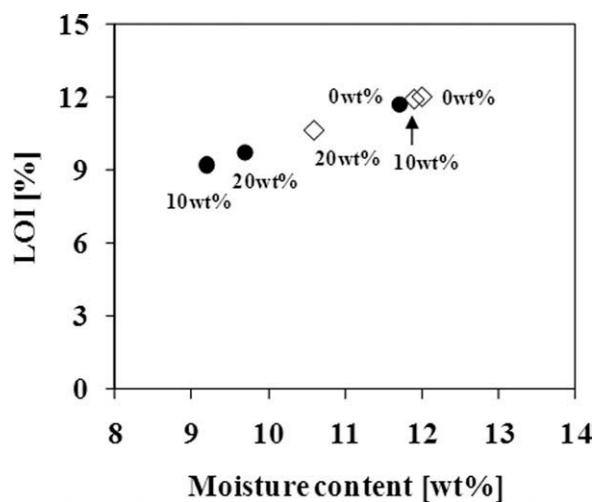
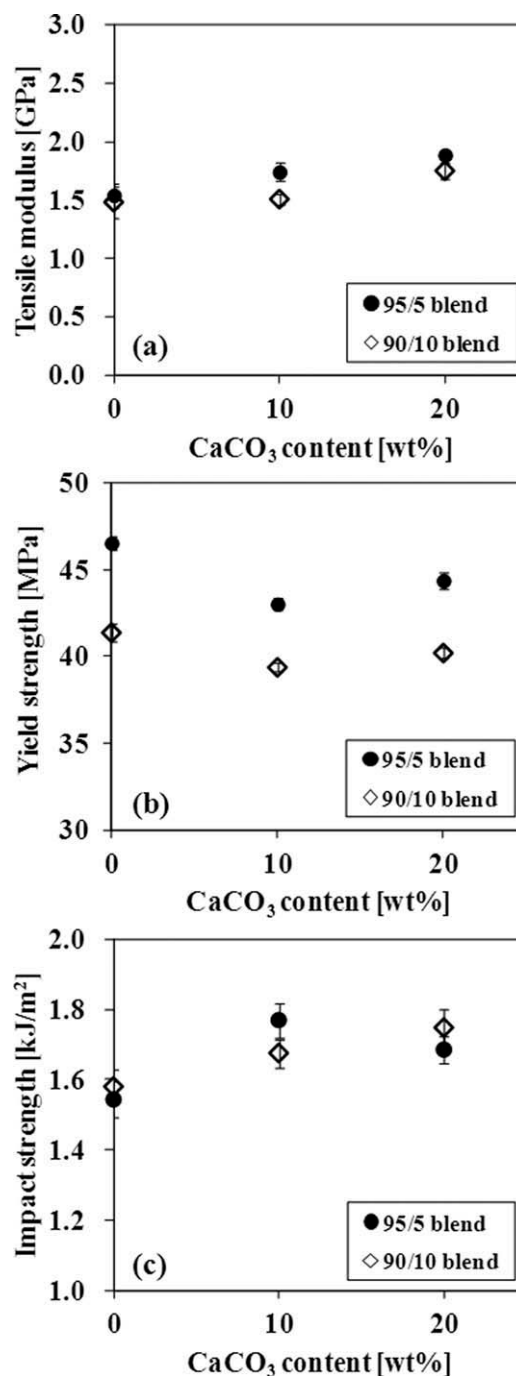
**Table VI.** Activation Energy from Kissinger and Kim-Park Model of Unfilled and CaCO<sub>3</sub> Filled 95/5 Blend and 90/10 Blend in Air

RPET/RPP blend	CaCO <sub>3</sub> (wt %)	Kissinger		Kim-Park	
		$E_a$ (kJ/mol)	$r$	$E_a$ (kJ/mol)	$r$
95/5	0	158.9	0.9907	162.0	0.9918
	10	175.7	0.9958	178.1	0.9963
	20	177.9	0.9900	180.1	0.9911
90/10	0	174.0	0.9954	176.4	0.9961
	10	202.2	0.9968	203.3	0.9972
	20	205.3	0.9907	206.8	0.9917

**Table VII.** LOI and Moisture Content of Unfilled CaCO<sub>3</sub> Filled 95/5 Blend and 90/10 Blend

RPET/RPP blend	CaCO <sub>3</sub> (wt %)	LOI (%)	Moisture content (wt %)
95/5	0	23.2	11.7
	10	20.3	9.2
	20	21.1	9.7
90/10	0	22.4	12
	10	19.4	11.9
	20	20.5	10.6

were between 21 and 23%, which could then be classified as slow burning materials. However, the LOI of CaCO<sub>3</sub> filled RPET/RPP blend was lower than the unfilled. The higher LOI in the unfilled blends could be due to the presence of higher moisture content in the blend, as shown in Figure 9, which could reduce its flammability. The effect of moisture content on thermal protective performance of heat-resistant fabrics was also discussed by Lee.<sup>38</sup> His research revealed that moisture enhances the thermal insulation of fabrics made with polybenzimidazole, aramid, and their blend. In addition, Tsvetkov et al.<sup>23</sup> have reported that water behave as inert diluents, which could evaporate from the surface of organic particles during combustion, therefore substantially depleting the oxygen supply and markedly reduce the rate of the combustion process. Moreover, it was observed in the unfilled specimen that the region under the flame would melt instantaneously to cause dripping, which prevented the flame from spreading towards other parts of the specimen. The incorporation of CaCO<sub>3</sub>, however, prevented this dripping thus causing the specimens to continue burning. It should be noted that flame retardants are generally added into polymers at high contents of up to 60 wt %. Therefore, it is thought that the amount of CaCO<sub>3</sub> incorporated into the

**Figure 9.** LOI as a function of moisture content of CaCO<sub>3</sub> filled RPET/RPP blend.**Figure 10.** Mechanical properties of CaCO<sub>3</sub> filled RPET/RPP blend: (a) tensile modulus, (b) yield strength, and (c) notched impact strength.

blends may be insufficient to dilute the combustible portion of the blends. In this study, CaCO<sub>3</sub> that was incorporated into the RPET/RPP blend could possibly act as a flame retarding material by producing CO<sub>2</sub> during combustion and therefore would dilute the oxygen source. However, it was observed that the incorporation of CaCO<sub>3</sub> could initially reduce the LOI values of the RPET/RPP blends, although these values would increase again at a CaCO<sub>3</sub> content of 20 wt %. A higher content of CaCO<sub>3</sub> increased the LOI since the amount of combustible

content would be reduced while the presence of CO<sub>2</sub> from the filler decomposition could aid in extinguishing the flame.

The thermal oxidative decomposition kinetic of the filled blends can also be useful to explain their flame resistance. The second step of thermal oxidative decomposition in the filled blends when exposed to air can be related to the deterioration of carbonaceous elements or char formed from the initial decomposition of organic substances. The presence of CaCO<sub>3</sub> would accelerate the decomposition of aromatic groups in the blend during degradation leading to faster formation of char, which would provide better flame resistance to the RPET/RPP blend. However, at low content of filler could not yield efficiency flame retardancy of the filled blends.

#### Mechanical Properties of Unfilled and CaCO<sub>3</sub> Filled RPET/RPP Blend

Figure 10 presents the mechanical properties of unfilled and CaCO<sub>3</sub> filled RPET/RPP blends. The incorporation of CaCO<sub>3</sub> enhanced the stiffness and impact performance of the blend. The increment of tensile modulus of CaCO<sub>3</sub> filled blend was due to the high rigidity of the filler particles whereas cavitation caused by the poor interfacial adhesion between fillers and the matrix could enhance their impact performances. The smaller dispersed phase size indicated good interfacial interaction between RPP and RPET, which enabled efficient transfer of energy especially during impact loading. Incidentally, the reduction in yield strength of CaCO<sub>3</sub> filled blends would also be due to the lack of interfacial adhesion between filler and the blend matrix. However, yield strength increased when increasing CaCO<sub>3</sub> contents, which indicated the reinforcing effect of CaCO<sub>3</sub> on tensile properties of the blends. It is also noteworthy that tensile properties of the 95/5 blends was higher than those 90/10 blends due to the low weight fraction of RPET in the former.

#### CONCLUSION

Morphological characteristics of compatibilized CaCO<sub>3</sub> filled RPET/RPP blends play an important role on thermal stability and mechanical properties of the blends. Smaller RPP dispersed phase size provided good thermal stability and excellent mechanical performance, especially when incorporated with CaCO<sub>3</sub>. RPP dispersed sizes of CaCO<sub>3</sub> filled 95/5 blends were lower, which obtained greater properties as compared to the 90/10 blends. The incorporation of CaCO<sub>3</sub> improved thermal degradation resistance of RPET/RPP blends by increasing activation energy for thermal degradation and decomposition kinetic and therefore reducing thermo-oxidative degradation. The Flynn-Wall-Ozawa model was useful in understanding the thermal degradation mechanism of the multicomponents of CaCO<sub>3</sub> filled RPET/RPP blend, particularly at the early stages of degradation. A multiple-step thermal decomposition characteristic was observed by using the Flynn-Wall-Ozawa model, which was attributed to the decomposition of different components at different periods of time. Kissinger and Kim-Park models provided similar activation energy results and, therefore, are equally reliable to provide good understanding of the final stages of the degradation. The incorporation of CaCO<sub>3</sub> acts as a barrier to

prevent penetration from volatile product and traps free radical during polymer decomposition. In addition, it was also responsible for accelerating the decomposition of the aromatic compounds leading to faster formation of char, which provided better flame resistance to the RPET/RPP blend. Nevertheless, the char formation of CaCO<sub>3</sub> was not enough for yield flame retardancy in these blends.

#### REFERENCES

1. Budrugaec, P. J. *Thermal Anal. Calorimetry* **2001**, *65*, 309.
2. Cooney, J. D.; Day, M.; Wiles, D. M. *J. Appl. Polym. Sci.* **1983**, *28*, 2887.
3. Gašparovič, L.; Koreňová, Z.; Jelemenský, Ľ. *Chem. Papers* **2010**, *64*, 174.
4. Girija, B. G.; Sailaja, R.R. N.; Madras, G. *Polym. Degrad. Stab.* **2005**, *90*, 147.
5. Kim, H.-S., et al. *J. Appl. Polym. Sci.* **2008**, *109*, 3087.
6. Kim, J. Y.; Kim, D. K.; Kim, S. H. *Polym. Compos.* **2009**, *30*, 1779.
7. Nguyen, L. H.; Gu, M. *Macromol. Chem. Phys.* **2005**, *206*, 1659.
8. Paik, P.; Kar, K. K. *Polym. Degrad. Stab.* **2008**, *93*, 24.
9. Sirin, K.; Dogan, F.; Balcan, M.; Kaya, I. *J. Macromol. Sci. A* **2009**, *46*, 949.
10. Tang, W.; Li, X.-G.; Yan, D. *J. Appl. Polym. Sci.* **2004**, *91*, 445.
11. Kim, S.; Park, J. K. *Thermochim. Acta* **1995**, *264*, 137.
12. [http://www.petbottle-rec.gr.jp/english/index\\_trend.html](http://www.petbottle-rec.gr.jp/english/index_trend.html). Accessed on August 20, 2009.
13. Heino, M., et al. *J. Appl. Polym. Sci.* **1997**, *65*, 241.
14. Pang, Y. X., et al. *Polymer* **2000**, *41*, 357.
15. Papadopoulou, C. P.; Kalfoglou, N. K. *Polymer* **2000**, *41*, 2543.
16. Goodarzi, V., et al. *J. Appl. Polym. Sci.* **2008**, *110*, 2971.
17. Guan, J.; Chen, G. *Fibers Polymers* **2008**, *9*, 438.
18. Huang, N.; Wang, J. J. *Anal. Appl. Pyrolysis* **2009**, *84*, 124.
19. Jiao, C.; Chen, X. *Polym. Eng. Sci.* **2010**, *50*, 767.
20. Karlsson, L., et al. *Polym. Degrad. Stab.* **2009**, *94*, 527.
21. Lecomte, H. A.; Liggat, J. J. *Polym. Degrad. Stab.* **2008**, *93*, 498.
22. Ren, Y., et al. *Front. Chem. China* **2009**, *4*, 136.
23. Tsvetkov, M. N., et al. *Pharm. Chem. J.* **1977**, *11*, 1087.
24. Xu, H.-J.; Jin, F.-L.; Park, S.-J. *B. Korean Chem. Soc.* **2009**, *30*, 2643.
25. Ogazi-Onyemaechi, B. C.; Leong, Y. W.; Hamada, H. J. *Appl. Polym. Sci.* **2010**, *116*, 132.
26. Chiu, H.-T.; Hsiao, Y.-K.J. *Polym. Res.* **2006**, *13*, 153.
27. Pracella, M.; Pazzagli, F.; Galeski, A. *Polym. Bull.* **2002**, *48*, 67.
28. Kim, H.-S., et al. *Eur. Polym. J.* **2007**, *43*, 1729.

29. Wang, F.-Y.; Ma, C.-C.M.; Wu, W.-J.J. *Appl. Polym. Sci.* **2001**, *80*, 188.
30. Doyle, C. D. *J. Appl. Polym. Sci.* **1961**, *5*, 285.
31. Flynn, J. H. *J. Thermal Anal. Calorimetry* **1983**, *27*, 95.
32. Di Lorenzo, M. L.; Errico, M. E.; Avella, M. J. *Mater. Sci.* **2002**, *37*, 2351.
33. Zaharescu, T., et al. *Polym. Bull.* **2002**, *49*, 289.
34. Rocco, J., et al. *J. Thermal Anal. Calorimetry* **2004**, *75*, 551.
35. Jipa, S.; Zaharescu, T.; Supaphol, P. *Polym. Bull.* **2010**, *64*, 783.
36. Rao, T. R. *Chem. Eng. Technol.* **1996**, *19*, 373.
37. Mishra, S.; Shimpi, N.; Patil, U. J. *Polym. Res.* **2007**, *14*, 449.
38. Young Moo, L.; Barker, R. L. *J. Fire Sci.* **1986**, *4*, 315.